Seismic performance of reinforced concrete frame structures strengthened with FRP laminates using a reliability-based advanced approach

Osama Ali, David Bigaud, Hassen Riahi

Seismic performance of reinforced concrete frame structures strengthened with FRP laminates using a reliability-based advanced approach

Submitted to <u>Composites Part B: Engineering</u>. Ed. Elsevier

Osama ALI[a], David BIGAUD[b*], Hassen RIAHI[b]

[a]*Civil Engineering Department at Faculty of Engineering-Aswan University, Egypt*

[b]*LARIS Laboratory, Angers University, 62 avenue Notre Dame du Lac, F-49000 Angers, France*

*Corresponding author.   David BIGAUD; orcid.org/0000-0001-8474-2885

E-mail: david.bigaud@univ-angers.fr ; Tel.:+33- 244 687 551

Bibliographical notes

Osama ALI is lecturer in the civil engineering department, faculty of engineering, Aswan University, Egypt. He holds his BSc degree in civil engineering from faculty of engineering, Aswan University. He awarded his MSc degree from structural engineering department, faculty of engineering, Cairo University (Egypt). The thesis entitled: Elastic analysis and Design of Pre-stressed composite girder. He received his PhD from Angers University, France, in 2012. PhD title is: Time-dependent reliability of FRP strengthened reinforced concrete beams under coupled corrosion and changing loading effects. His research activities in the areas of structural reliability of RC structures, finite element analysis of RC structures, strengthening and repair of RC structures using FRP composites, structural optimization, corrosion of steel reinforcement embedded in concrete and performance of RC structures under seismic loads.

David BIGAUD is specialized in polymer and composite materials (Eng. 1993 from ITECH-Lyon). He obtained his PhD in 1997 on the topic of the multi-scale modeling of textile-reinforced composite materials. From 1998 to 2005, he was Associate Professor and has developed research on 3D textile-reinforced composites for civil engineering, transportation and aeronautical applications. In September 2005, he was promoted to a position of full Professor at the University of Angers. He develops there in Angers research activities on reliability and decision making about safety of systems. His research has resulted in many publications in several international journals. His research interests are related to the field of civil engineering and with emphasis on structures: pathology, materials, technical management and design of structures.

Hassen RIAHI Ph.D. in mechanical and civil engineering, is an associate professor at Angers University in France since 2014. His research interests the development of numerical models to solve the problem of the curse of dimensionality frequently encountered in uncertainty propagation though mechanical models. The concerned domains are mainly, fatigue of materials, fracture mechanics and structures subjected to seismic loading.

Seismic performance of reinforced concrete frame structures strengthened with FRP laminates using a reliability-based advanced approach

Abstract:

Effectiveness of applying FRP-strengthening to enhance the seismic performance of a RC frame structure is studied in this paper. The performance is expressed in term of reliability which implies calculation of the probability to reach the required level of performance under specified loadings and environmental conditions. The proposed approach was applied to a typical three-storey RC frame structure. Two strengthening configurations are compared: applying flexural FRP-strengthening to members – beams/columns – and/or applying FRP-confinement to columns of the structure. Seismic reliability assessments are presented in term of fragility estimates which involves performing nonlinear time history analysis to record the maximum lateral top drift of the RC frame structure under seismic loadings. This analysis is carried out using finite elements method. To reduce the computational effort, an efficient meta-modelling method based on Polynomial Dimensional Decomposition PDD in conjunction with the Monte-Carlo Simulation is developed. Results of simulations demonstrate the efficiency and computational advantages of the proposed method for the seismic reliability assessment of RC frame structures. Furthermore, the results confirm a significant increase in reliability of RC-frames subjected to seismic due to FRP-flexural/FRP-confinement strengthening especially in case of applying FRP-flexural strengthening.

1. Introduction:

Externally bonded (EB) Fibre Reinforced Polymer (FRP) Composite material (laminates or sheets) have been used for over two decades to strengthen reinforced concrete RC structures. This relatively new strengthening technique is a widely accepted strengthening alternative around the world. The rise of FRP composites in strengthening applications of RC structures can be attributed to their high strength, resistance to corrosion, light weight and ease of application (American Concrete Institute Committee 440 [1]). It is well

proven that FRP-strengthening can improve both flexural and shear resistances of RC structures [2-7]. In addition, concrete columns gains more strength when confined with FRP composites [8-11]. Other authors have carried out or reported experimental works that show the significant enhancement of yield load, stiffness and energy dissipated capacity under cyclic loadings [12-14].

EB-FRP technique can be used not only to sustain static loads but also to support seismic/lateral loads in RC frame structures. Seismic strengthening can be performed by applying FRP flexural laminates to the most tensioned fibres of RC of beams/columns or/and by improving axial strength of concrete columns when confined by FRP wraps. Thus, an overall seismic enhancement in performance of RC frames can be achieved such as increasing lateral shear strength and/or reducing top lateral drift [15-17]. Del Zoppo *et al.* [18] and Di Ludovico *et al* [19] studied experimentally and analytically FRP-retrofitting of a full scale two and three-storey RC structure under seismic actions with varying intensities. FRP confinement was applied to columns while flexural strengthening was applied to beams. Their results suggested a considerable increase in capacity and less damage. Similar observations were achieved by Garcia *et al* [20], as they studied the effect of confinement/flexural FRP-strengthening on two full-scale two-storey RC frames subjected to different shaking levels. According to their results, a desirable sway was investigated with significant increase in columns capacity. Eslami and Ronagh [21] have carried out a numerical investigation into the efficiency of glass fibre reinforced polymers in improving the seismic performance of an eight-storey moment resisting reinforced concrete building. Their retrofitting strategy aimed to provide both columns and beams with more ductility of plastic hinges at beam/column ends and energy dissipation instead of increasing the lateral strength. Their results confirmed that GFRP wraps can significantly improve the seismic performance as RC frame could resist mush higher ground motions.

It is worth mentioning that deterministic analytical/numerical models cannot provide measure the level of safety of FRP strengthened structural members when including the statistic nature of design variables (material properties, section geometry and loads) in the analysis. Such probabilistic approaches now underlie conventional international design codes. In the last decades, structural reliability algorithms were used in many studies to accurately evaluate the increase in safety level when applying FRP strengthening to structural elements (made of RC, wood or steel) under static loads [22-25]. Unfortunately, most of these studies do not

cover the applications of FRP strengthening RC frame structures under earthquakes. Thus, reliability of FRP strengthened RC frames under earthquakes need to be handled. This can help in evaluating for what level EB-FRP strengthening can enhance structural reliability/safety of RC frames under actual seismic loads. From this point of view, the proposed study aims to implement structural reliability analysis of the EB-FRP flexural/confinement strengthening of RC frame under seismic actions.

Generally, in probabilistic terms, reliability can be expressed in two different forms: the reliability index β or the frequency of failure P_f. An oversimplified but clear manner to explain what is the first form β is illustrated in Fig. 1. β can be regarded as the ratio between the mean value μ_M and the standard deviation σ_M of the margin (defined as the difference between Resistance and Stress) statistical law. There is an approximated relation between β and P_f: $P_f \approx \Phi(\beta)$, where Φ is the standard normal distribution law. The reliability index β can be investigated using, for example, First/Second Order Reliability Method *FORM/SORM*. The use of these methods requires an explicit analytical formula of the limit state function and its corresponding differentiations with respect to its random variables. This limit state function is the multidimensional curve for which the margin (or the difference between applied stresses and structural or material resistance) is equal to zero. Finally, a reliability study consists in an optimization problem and aims at estimating the probability that the margin is lower than zero. If an analytical formulation of the limit state function exists (or an approximation) the frequency of failure P_f can be estimated using simulation techniques, e.g. Monte-Carlo simulation, which require a huge number of model calls. But, practically, implementation of reliability studies is quite complex because the optimization problem to deal with may be a high-dimensional one and the components (or variables) of the limit state function basically may evolve during time or with geometrical and/or material non-linearity [26].

➔ *[Figure 1: Naïve illustration of two reliability indicators. Near here]*

If, on top of that, no analytical formulation is possible, such as in the case of the use of FEM, a huge number of simulation calls, highly time consuming, is required. To override these drawbacks, a response function/meta-model can be constructed by performing a limited number of relevant FEM calls. Many methods of response functions construction had been developed in previous studies such as Quadratic Response Surface *QRS* method, which can, to some extent, fit the points of design of experiments locally and

required many repetitions to reach convergence. Another type is the Fuzzy fitting algorithms such as Neural Network application *NN*, Support Vector Machine …etc. Generally, such these algorithms require a high number of training data, high time cost in training process and number of variables is limited to 6-8 [26]. Recently, response functions based on the analysis of variance have increasingly been used such as Stochastic Response Surface method SRSM and Polynomial Dimension Decomposition PDD [27].

In the present study, a relevant approach for the probabilistic assessment of reinforced concrete frame structures strengthened with FRP laminates under seismic loading is proposed. Nonlinear finite element time-history analyses were carried out to evaluate the required response – maximum lateral top drift on the entire loading duration – of an existing/FRP-strengthened RC frame. Seismic reliability, of serviceability limit state, was defined in term of fragility. Face to the huge number of simulations required to estimate failure probabilities, a Polynomial Dimension Decomposition strategy is chosen for that it is considered more economic in the number of FEM calls and that it represents accurately the true function in high dimension problems. To go further, a sensitivity analysis is performed to evaluate the importance of each random variable considered in the reliability study and seismic design recommendations are suggested.

2. *Probabilistic Seismic Fragility.*

Structural seismic performance can be presented in the form of fragility curves which correspond to the limit state function $G = R(X,t) - S(X,t) < 0$, where R is the structural Resistance (or capacity) and S is the Stress (or demand). Both resistance and stress are function of time t. X is a set of random variables representing material, geometrical, loading parameters variability…etc. In probabilistic terms, reliability of a structure (and conversely, fragility) can be considered as the conditional probability that stress does not exceed (conversely, exceeds) the resistance performances for a given ground motion intensity. Such performances are the maximum acceleration, velocity, displacement, spectral acceleration… etc. Previously, many research works in the literature on the topic of seismic reliability or fragility of RC structures were developed [28-32], but very few of them deal with the effect of FRP-strengthening on the enhancement of these reliability or fragility.

In the present study, the serviceability limit state *SLS* – operational – is considered. In this case, the stress S is expressed in term of maximum lateral top drift Δ_{max} of the frame during the entire ground motion - thus,

the explicit time-dependence of the limit state G no more needs to be reflected on time is diminished [33] – and the resistance R is a given allowable deterministic value of the lateral top drift Δ_{all} (following Eurocode 8 (EC8) [34], Δ_{all} equals to 5‰ of the total height of the building). The final form of the limit state function can be written as:

$$G = R(X,t) - S(X,t) = R(X) - S(X) = \Delta_{all}(X) - \gamma_m \Delta_{max}(X) \tag{1}$$

where γ_m is a random variable taking into account the model error and was considered to be normally distributed with mean value and standard deviation equal to 1.01 and 0.046 respectively as recommended by Vu and Stewart [35].

Presently, the study aims to approximate the lateral top drift Δ_{max}, and *a fortiori* the limit state function G, using Polynomial Dimension Decomposition, PDD. Δ_{max} being estimated from FEM simulations. Then after, the statistic dispersion of the influencing parameters will be considered. Finally, Monte Carlo simulations on the approximated function, called also "response surface/Metal model" obtained from PDD, is applied to calculate the fragility F (or the probability P_f that $\gamma_m \Delta_{max}(X)$ is greater than $\Delta_{all}(X)$ under a given ground motion:

$$P_f = Pr(\gamma_m \Delta_{max}(X) \geq \Delta_{all}(X)|ground\ motion\ intensity) \tag{2}$$

To represent a complete fragility curve, multiple value of Δ_{all} will be considered. Finally, a structure can be considered as well-designed if its fragility F or reliability index β is smaller or greater, respectively, than an acceptable or target value. No specification about this target value in the case of seismic loading is provided in EC8 [34]. For guidance purpose, we can refer to Eurocode 0 (EC0) [36]. For a service life of 50 years, it gives a maximum value of acceptable reliability index equal to 3.8 for fatigue or cyclic loadings (in fact, EC0 specifies a range between 1.5 and 3.8 depending on degree of inspectability, reparability and damage tolerance, but here, we consider the worst-case scenario. Indeed, higher is the value of β, lesser is the acceptable failure probability P_f). For their part, Hirataï and Ishikawa [37] proposed to choose an intermediate value of 2.4.

3. Case study

3.1 Reinforced concrete frame structures strengthened with FRP laminates

In the present study a typical symmetrical three-storey RC frame with structural configurations properties shown in Fig. 2a and Table. 1 was considered. The given frame configurations was originally studied by Buratti *et al*. [30] as RC frame. In the numerical model, in order to account reasonably the material nonlinearity, all beams and columns will be divided into nine and six segments in their longitudinal dimension respectively as shown in Fig 3a. Full restraints were assumed at the base of the frame. It was assumed that FRP laminates used in flexural strengthening are anchored in end regions. Thus, all FRP-end debonding failure modes can be totally neglected.

➔ *[Figure 2: a) Three-storey RC Frame configuration (from [30]). b) considered FRP strengthening schemes. Near here]*

➔ *[Table 1: Cross-sections geometry of RC frame. Near here]*

Two strengthening options were applied: the first is FRP-confining strengthening which is applied to the columns of the RC frame only, while the second option is FRP-flexural strengthening which is applied to beams and columns of the RC frame according to the schemes shown in Fig. 2b. Thickness of FRP laminates used for confining and flexural strengthening options were taken equal to $t_{FRP,conf}$ =1 mm and $t_{FRP,flex}$ =0.7 mm respectively. Width of FRP laminates used in flexural strengthening was taken equal to 225 mm. Fragility curves will be constructed for the cases given in Table 2. The choice of corner radius r_c of a value equal to 30 mm was considered according to Wang & Wu [38] and Sharma *et al* [33]. The authors suggested this value to be the minimum effective corner radius and our intent is to consider the worst situations.

➔ *[Table 2: Description of the studied cases. Near here]*

3.2 Material behaviour and failure modes

The stress-strain relationship of unconfined concrete in compression is described by the nonlinear relationship given in the following equation (from [40]):

$$\sigma_c = f_c' \left[\frac{2\epsilon_c}{\varepsilon_{c_o}} - \left(\frac{\epsilon_c}{\varepsilon_{c_o}} \right)^2 \right] \tag{3}$$

where f_c is the concrete compressive strength, ε_{co}; $= 2f_c/E_c$, indicates the strain corresponding to the peak

stress of the unconfined concrete (see Fig. 3a) and E_c represents the initial tangent modulus of the concrete.

The stress strain for FRP-confined concrete is divided into two ascending parts (see Fig. 3a): the first part is

like that of unconfined concrete from zero to a stress equal to f_c while the second part is linear until the

ultimate strength of confined concrete stress f_{cc}. Therefore, concrete member under axial compression could

gain more axial stiffness due to FRP confinement effect. Thus, if the same level of loading is adopted, an

overall increase in the flexural stiffness and, consequently, decrease in deformations of these members could

be achieved. The ultimate strength of FRP-confined concrete f_{cc} and the corresponding strain ε_{cc} are given,

respectively, by (from [40-41]):

$$f_{cc} = f_c' \left(1 + 2.15 \frac{f_l}{f_c'} \right) \tag{4}$$

$$\varepsilon_{cc} = \varepsilon_{c_o} \left(2 + 15 \frac{f_l}{f_c'} \right) \tag{5}$$

where f_l is the lateral confining pressure which for rectangular sections can be calculated with the

following equation:

$$f_l = k_s \frac{2 f_{FRP} t_{FRP,conf}}{0.5(b + h)} \tag{6}$$

where f_{FRP} and $t_{FRP,conf}$ are the rupture strength and thickness of confinement FRP material respectively. b

and h are width and height of RC section. k_s is shape factor that is equal to the ratio of the effective confined

area to the gross concrete area enclosed by FRP and is expressed as (from [40-41]):

$$k_s = \left[1 - \frac{(b - 2r_c)^2 + (h - 2r_c)^2}{3bh} - \rho_s \right] / (1 - \rho_s) \tag{7}$$

where r_c is the corner radius and ρ_s is the longitudinal steel ratio. Transverse steel confinement is

neglected as the objective of the present study is to examine the enhancement in seismic reliability in applying

FRP strengthening to an existing RC frame. This assumption is reasonable as lack of stirrups amount is a characteristic feature for old RC building.

It is assumed that concrete is linearly elastic in the tension region. Beyond the tensile strength, f_{ct}=0.3 $(f_c)^{2/3}$ (CEB-FIB Model Code 1990 [42]), the tensile stress decreases linearly as the principal tensile strain increases as shown in Fig. 3b. Ultimate failure from cracking is assumed to occur when the tensile strain exceeds the value ε_{ut}=2G_f/ f_{ct}, where G_f is the fracture energy which is dissipated during the formation of a crack and was taken as (from [43]):

$$G_f = 2.5\alpha_o \left(\frac{f_c'}{0.051}\right)^{0.46} \left(1 + \frac{d_a}{11.27}\right)^{0.22} wc^{-0.3}$$
(8)

where α_o=1.44 for crushed or angular aggregate diameter. d_a (mm) is the maximum aggregate size. In the present study, it will be assumed that d_a=32 mm. wc=0.45 is the water-to-cement ratio in the concrete mix. The constitutive model used to simulate the steel reinforcement was the classical metal elastic-perfectly plastic model, while linear elastic behaviour up to failure was assumed for FRP laminates. Perfect bond between concrete and both steel reinforcement and FRP laminates was assumed.

➔ *[Figure 3: Concrete stress-strain curves. Near here]*

Table 3 gives all probabilistic properties of the random variables considered in the fragility analysis. The considered variables relate to material and loading properties. FRP-geometrical properties were considered as deterministic variables as they have insignificant effect in reliability [2,23-24].

➔ *[Table 3: Probabilistic parameters of random variables. Near here]*

4. *Numerical assessment of seismic reliability.*

As already mentioned, stochastic non-linear time history analyses are required to obtained fragility curves. These analyses were carried out using the computer Abaqus/standard package [44] to evaluate the required

response – maximum lateral top drift on an entire seismic loading duration - of an existing/FRP-strengthened RC frame. They are basically implemented by considering material and geometrical nonlinearities.

Rayleigh-proportional damping mass and stiffness constants, a_o and a_1 respectively, were formulated for each FEM run by estimating the first three natural frequencies as: $a_o=2\zeta\omega_1\omega_3/(\omega_1+\omega_3)$ & $a_1=2\zeta/(\omega_1+\omega_3)$, ζ is the damping ratio, ω_1 and ω_3 are the first and third frequencies respectively [45]. Formulation assures that reasonable damping at the second frequency, while for higher frequencies the third would produce a very high damping that be essentially eliminated due to their illogical damping values.

4.1 Finite Element Modelling

Nonlinear time history analysis of the RC frame was carried using Abaqus/Standard finite element program. Beams and columns of RC frame were modelled using 2-dimensional beam element (B21) while longitudinal steel reinforcements and flexural FRP laminates were modelled using rebar option. In the numerical model, all beams and columns were divided into nine and six segments in their longitudinal dimension respectively as shown in Fig 4a. When applying FRP confinement strengthening, it is assumed that confinement effect will be applied to columns of RC only while beams were assumed to be unconfined, as slabs prevent wrapping of FRP-laminates around beams. Two approaches are available in Abaqus/Standard to predict the behaviour of concrete: smeared crack and plastic damage models. The plastic damage model was selected for this study since it has higher potential for convergence compared to the smeared crack model [44]. The cross sections of beams and columns have been divided into nine integrations points. The system's masses are assumed to be concentrated at each storey level (from loads applied to beams).

Two finite element loading steps were performed; the first step is static which includes the application of dead and live loads only while the second step is a time history analysis due to ground acceleration. Fig. 4b shows the ground acceleration that was applied at the base points of the frame. The considered ground motion has a Peak Ground Acceleration of 0.33g and a total duration of 30 seconds.

As a sample of FEM runs, Fig. 4c presents the lateral top drift calculated over the entire duration of the seismic action corresponding to the reference point c. The maximum lateral top drift, the desired PDD response $y(c_1 \ldots c_N)$, was recorded to 43.51mm at a time of 14.1sec.

4.2 Polynomial Dimensional Decomposition PDD

4.2.1 General aspects

Polynomial Dimensional Decomposition PDD, also called High Dimensional Model Representation HDMR, is an efficient meta modelling approach dedicated to highly nonlinear complex input-output problems. Generally, the determination of the reliability value requires a transformation of the limit state/response function from the physical space $G(X)$ to the standard random space $K(U)$. $X= \{x_1,..., x_N\}^T$ is the set of random physical variables in the reliability problem and $U= \{u_1,…, u_N\}^T$ is the corresponding set of X in the normalized standard space. The transformation from the physical space X to the standard space U is carried out through a probabilistic transformation T: $X=T(U)$ or $U=T^{-1}(X)$, such as the Nataf distribution [46] which is used in this work. Establishing the response function $K(U)$ – where U is an input vector of N variables in the standard space - using PDD requires the definition of a reference point – $c=\{c_1,…,c_N\}^T$. The later can be defined as the mean point, which gives accurate results when dealing with statistical moments or sensitivity analysis [27]. However, if the study is focused on reliability analysis, is more suitable to define the reference point as the design point (i.e. the most probable failure point), which can be easily obtained through First Order Reliability Method [26]. In the proposed study, the origin of the standard normalized space, *i.e.* where all variables are equal to their respective mean value, was defined as this reference point. According to the PDD method [27, 47], the S-dimensional approximation $\widehat{K_S}$ of the mechanical response K, reads:

$$\widehat{K_S}(U) \cong y_o + \sum_{i=1}^{N}\sum_{j=1}^{m} \alpha_{ij}\psi_j(u_i) + \sum_{i_1=1}^{N-1}\sum_{i_2=i_1+1}^{N}\sum_{j_1=1}^{m}\sum_{j_2=1}^{m} \beta_{i_1i_2j_1j_2}\psi_{j_1}(u_{i_1})\psi_{j_2}(u_{i_2})$$

$$+\sum_{i_1=1}^{N-2}\sum_{i_2=i_1+1}^{N-1}\sum_{i_3=i_2+1}^{N}\sum_{j_1=1}^{m}\sum_{j_2=1}^{m}\sum_{j_3=1}^{m} \gamma_{i_1i_2i_3j_1j_2j_3}\,\psi_{j_1}(u_{i_1})\psi_{j_2}(u_{i_2})\psi_{j_3}(u_{i_3}) + \cdots \qquad (9)$$

$$+\sum_{i_1...i_S;i_1<i_2<\cdots<i_S}^{N-S+1}\sum_{j_1=1}^{m}\cdots\sum_{j_S=1}^{m} C_{i_1...i_S\,j_1...j_S}\prod_{k=1}^{S}\psi_{j_k}(u_{i_k})$$

where ψ_j is a unidimensional orthogonal j-order polynomial in normalized form. S is the order of PDD. m is the maximum order of polynomial ψ_j. N is the number of variables.

In the present study Hermite polynomials H_j were chosen to express ψ_j function as:

$$\psi_j = \frac{H_j}{\|H_j\|} = \frac{H_j}{\sqrt{j!}}, j = 1, 2, \ldots, m \tag{10}$$

The expansion given in Eq. 9 approximates $K(U)$ when the parameter $m \to \infty$. Practically, y_o, α, β, γ, ...C are the unknown coefficients to determine. But, in the case of high-dimensional problems, a huge number of FEM calls will be required to estimate them. Dealing with this problem, and aiming to decrease computation time, Rahman [47], and, Xu and Rahman [48] have suggested to estimate these coefficients using dimension reduction integration method. The expansion is truncated to a certain order and the coefficients can be expressed as:

y_o

$$= \sum_{k=0}^{R} (-1)^k \binom{N-R+k-1}{k} \sum_{\substack{k_1 \ldots k_{R-k}; k_1 = 1 < \cdots < k_{R-k}}}^{N-R+k-1} \int_{\Re^{R-k}} y\left(c_1 \ldots c_{k_1-1}, c_{k_1}, c_{k_1+1} \ldots c_{k_{R-k}-1}, c_{k_{R-k}}, c_{k_{R-k}+1} \ldots c_N\right)$$
$$\times \prod_l^{R-k} \phi_{k_l}(u_{k_l}) dx_{k_l} \tag{11}$$

$C_{i_1 \ldots i_S j_1 \ldots j_S}$

$$= \sum_{k=0}^{R} (-1)^k \binom{N-R+k-1}{k} \sum_{\substack{k_1 \ldots k_{R-k}; k_1 = 1 < \cdots < k_{R-k}}}^{N-R+k-1} \int_{\Re^{R-k}} y\left(c_1 \ldots c_{k_1-1}, c_{k_1}, c_{k_1+1} \ldots c_{k_{R-k}-1}, c_{k_{R-k}}, c_{k_{R-k}+1} \ldots c_N\right)$$
$$\times \prod_l^{R-k} \psi_{j_l}(u_{i_l}) dx_{k_l} \prod_l^{R-k} \phi_{k_l}(u_{k_l}) du_{k_l} \tag{12}$$

where R is the dimensional reduction order of the integration that can be carried out through numerical integration method. ϕ is the Gauss probability density function with a mean value equal to zero and standard deviation is unity.

The "economy" of computation time induced by PDD depends on the truncation order R, on the number of uncertain parameters N and on the number of integration points n. It can be defined as the ratio of the number of FEM calls required by the PDD method, *i.e.* $\sum_{k=0}^{k=R} C_N^{R-k}(n-1)^{R-k}$, to the number of FEM calls required by the fully tensor product quadrature rule, *i.e.* n^N [47]. The PDD method is obviously very useful (and efficient) to compute high-dimensional integrals. For example, in our case for which $N = 9$ and with $R = 2$, $n = 5$, this ratio is around 3000. Considering the time required for each FEM calls (see §4.2.2 below), PDD is a necessary condition for dealing with complex simulations as in our case.

In the present study, Gauss-Hermite quadrature rule with n integration points on each dimension was considered. It is worth mentioning that the accuracy, also, of PDD expansion function depends on the choice of the parameters S, R, n, and m. The parameter R should be selected in such manner that $S \leq R < N$. It is generally recommended to be taken equal to the PDD order S. In addition, the number of integration points n can be assumed, while m can be evaluated using try-and-error procedure starting from $m = 1$ to $m = n-1$, until accuracy of PDD function is achieved. Otherwise n must be updated to a higher value [47]. Fig. 5 shows the computational procedure for constructing PDD function.

➜ *[Figure 5: Computational procedure for the establishment of dimensional polynomial decomposition function. Near here]*

Following procedure described in Fig. 5, the parameters – R, S, n & m – required for PDD were found to be equal to $R = S = 2$, $n = 5$ and $m = 4$. To assess generalization capability of the approximate response surface built with these parameters (R, S, …), we choose points in the normalized standard space out of the design of experiments used for the polynomial constants evaluation and compare values of lateral top drift $\Delta_{max}(U)$ provided by FEM simulations and calculated from the response surface. The elementary integrals in equations (11) and (12), resulting from the dimension reduction process, are computed using 10th order Gauss-Hermite cubature rule. Fig. 6 shows the results of FEM and *PDD* at the chosen verification points on each random variable. We can conclude that PDD can give a response surface ($\widehat{K}_S$ with $R = S = 2$, $n = 5$ and $m = 4$) that accurately predicts the lateral top drift Δ_{max}. and on which to carry out Monte Carlo simulations.

➜ *[Figure 6: Validation of polynomial dimensional decomposition PDD function. Near here]*

In addition to the accuracy achieved using PDD, the number of FEM calls is an important factor which controls efficiency of the used method. In our cases, to carry out the reliability analysis needs at least 10^5 Monte Carlo simulations. Thus, too many FEM calculations are required and computing costs will be prohibitive without using the PDD function (10^5 x 6.8 min $\rightarrow$ 472 days). 6.8 min is the average computing time of a FEM call, which was found to range between 2.75 and 16.82 min. In the other hand, to use PDD requires 266 FEM calls to build, for instance, the above-mentioned $\widehat{K}_S$ function with $R = S = 2$, $n = 5$ and $m = 4$, for the first case ("Ref"). The total average computing time is about 30 hours. When compared with computing time without using PDD (472 days), this reflects absolute necessity and efficiency of the proposed approach coupling FEM simulations, PDD approximation and Monte Carlo simulations.

4.2.2 *Thorough interpretation of the PDD results and sensitivity analysis*

The statistical moments of the response (here, the lateral top drift) obtained by using polynomial dimensional decomposition method can be directly calculated from the constants obtained from Eq. 11 and Eq. 12. In this context, the statistical moments can be easily obtained by applying the Esperance E[.] to Eq. 9 and exploiting the orthogonality of the Hermite polynomials. The mean and variance of the response can be expressed as (from [27]):

$$\hat{\mu}_{K_S} = E[\widehat{K}_S] = y_o \tag{13}$$

$$\hat{\sigma}^2_{K_S} = E\left[(\widehat{K}_S - y_o)^2\right] = \sum_{k=1}^{S} \sum_{i_1=1}^{N-S+1} \cdots \sum_{i_S=i_{S-1}+1}^{N} \sum_{j_1=1}^{m} \cdots \sum_{j_S=1}^{m} C_{i_1 \ldots i_S \, j_1 \ldots j_S} \tag{14}$$

We can also use result of PDD to derive the total Sobol sensitivity indexes, $\widehat{S}^T_{i,S}$. They can be determined by carrying out a post treatment of PDD constants and can be expressed as (from [21, 49-50]):

$$\hat{S}^T_{i,S} = \hat{S}_{i,S} + \sum_{i_1 \neq i_2} \hat{S}_{i_1 i_2,S} + \sum_{i_1 \neq i_2, i_2 \neq i_3, i_2 < i_3} \hat{S}_{i_1 i_2 i_3,S} + \cdots \tag{15a}$$

where, $\tag{15b}$

$$\hat{S}_{i,1} = \frac{1}{\hat{\sigma}_{y,S}^2} \sum_{j=1}^{m} \alpha_{ij}^2 \; ; \; \hat{S}_{i_1 i_2,2} = \frac{1}{\hat{\sigma}_{y,S}^2} \sum_{j_1=1}^{m} \sum_{j_2=1}^{m} \beta_{i_1 i_2 j_1 j_2}^2 \; ; \; \hat{S}_{i_1 i_2 i_3,3} = \frac{1}{\hat{\sigma}_{y,S}^2} \sum_{j_1=1}^{m} \sum_{j_2=1}^{m} \sum_{j_3=1}^{m} \gamma_{i_1 i_2 i_3 j_1 j_2 j_3}^2$$

$$\hat{S}_{i_1 \dots i_S, S} = \frac{1}{\hat{\sigma}_{y,S}^2} \sum_{j_1=1}^{m} \dots \sum_{j_S=1}^{m} C_{i_1 \dots i_S j_1 \dots j_S}^2$$

5. *Results and discussion on the effect of strengthening upon seismic reliability*

In reliability terms, the objective of strengthening is to reduce damage probability, P_f (Eq. 2), under allowable or high values of lateral top drift (the demand). Herein, in order to evaluate strengthening effect on the lateral top drift, a reference value of allowable lateral drift Δ_{all}, equals to 5 ‰ of the total height of the building H_T was assumed. Referring to the proposed case of study where $H_T = 9$ m, $\Delta_{all,euro} = 45$mm.

Following procedure presented in §4.2 and Fig. 5, and as already mentioned, we approximate the limit state function $G(X) = K(U)$ by a polynomial response surface $\widehat{K_S}(U)$ with a truncation order R and PPD order S equal to 2 and a number of integration points n equal to 5. The mean and variance of maximum lateral top drift Δ_{max} in Fig. 7. It is obvious that the different considered strengthening techniques could improve the reliability of the RC frame not only by decreasing the mean value but also by decreasing the variance of lateral drift. Globally, flexural strengthening is the most influencing technique as it gives relative reduction of mean and standard deviation equal to 6.5% and 28.6% respectively. Evidently, more enhancement in the statistical moments may be reached when applying FRP composites with high modulus or/and thickness (parametric perspective analysis may be developed).

➔ *[Figure 7: Mean and standard deviation of lateral top drift (mm) of the different cases considered. Near here]*

➔ *[Figure 8: Sobol sensitivity indices of random variables included in PDD function. Near here]*

As far as Sobol indexes are concerned, the total sensitivity indexes obtained from Eq. 13, Eq. 14 and Eq. 15 are presented in Fig. 8. We observe that dead load DL, concrete compressive strength f'_c, live load LL and model error γ_m are the most important random variables that affect the reliability analysis. Steel yield stress f_y

and damping ratio ζ slightly affect the analysis especially in case of flexural strengthening. FRP properties f_{FRP}, E_{FRP} and steel modulus E_s have a negligible effect and are strongly recommended to be considered as deterministic, which can strongly reduce the number of implicit mechanical model calls in the subsequent uncertainty propagation analysis, such as reliability study for instance. In addition, based on these results the empirical design model commonly used in the design codes can be strongly simplified. Indeed, the FRP properties f_{FRP}, E_{FRP} and steel modulus E_s, in our case, can be discarded. Consequently, the resulting empirical model will be more suitable for engineering computations. Finally, the partial safety factors associated to the non-important parameters (i.e. from a probabilistic point of view) can be easily calibrated, since their respective values can be fixed to 1.

Monte Carlo simulations are next carried out on polynomial response surface $\widehat{K_S}(U)$. One of the output of these simulations are the probability density functions *PDF* of the maximum lateral top drift for each case of study referred in Table 2. It can be noted in Figure 9 that the *PDF* is not centred/ non-symmetrical and is difficult to be fitted with any analytical density (such as Gauss, Lognormal, or Weibull distributions). This may be due to nature of seismic loading under probabilistic analysis, which can produce high repetitions (density), as shown in figure 9, for more than one lateral drift during the duration of loading. Such this observation may be important when proposing maximum allowable drift in design codes - based on safety margin definition - considering some regional attributes of seismic load nature such as load duration/intensity.

A multimodal distribution may fit the general shape of the lateral top drift PDF. We notice that FRP-strengthening causes a decrease in top drift statistical moments, but the most significant decrease is observed for the standard deviation when applying FRP flexural strengthening. So, the FRP flexural strengthening technique can be strongly recommended in order to reduce top drift, than FRP confining technique of RC frames, to match code requirements.

➜ *[Figure 9: Density function PDF of lateral top drift Δ_{max} (mm). Near here].*

Fig. 10a and 10b show the fragility curves obtained using PDD for the different strengthening configurations of Table 2. As mentioned before, fragility analysis is performed using Monte-Carlo

simulations based on 10^5 calls of the analytic PDD model. It can be noted that all the considered FRP-strengthening configurations show a significant variation in fragility curves with respect to the reference case ("Ref"). On one hand, reductions of the damage probability of 31.5% and 16.3% are observed when applying FRP-flexural and FRP-confining strengthening respectively compared to the reference case ("Ref"). Therefore, it could be emphasized that applying FRP-flexural strengthening is more effective and can reduce with a factor two (from $P_f = 0.2175$ to $P_f = 0.1150$) until eventually reaching the target value, $P_{f,T}=0.1$, recommended by the Joint Committee on Structural Safety [51]. Herein, the main strengthening concern is to increase the flexural stiffness of the RC frame and, consequently, to decrease the lateral drift. This can explain the weak role of FRP confining in reducing the lateral drift, as it does not improve directly the flexural stiffness but by increase the axial stiffness of concrete, which, evidently, could not provide the same effect as FRP flexural strengthening technique. On the other hand, it can be observed in Fig. 10a that rounding the corners of RC section, $r_c=30$mm, could slightly reduce the damage probability.

➔ *[Figure 10: Fragility curves. Near here]*

Fragility curves can be viewed in a different way and be used to determine what should be the regulatory allowable lateral drift Δ_{all} for a given fragility (see right-hand side of Fig.10b). In the reference case "Ref", without strengthening, if we consider a target reliability index $\beta = 1.5$, the lowest target value found in Eurocode 0 [30] for fatigue or cyclic loadings, Δ_{all} should be 30 mm. It means that if the maximum actual lateral top drift is higher than 30 mm, the probability of damage P_f of the three-storey building under consideration becomes too high for a service life of 50 years (higher than 6.7×10^{-2}); this risk is unacceptable. As the prescribed lateral top drift is 45 mm, we can state here that the building, without strengthening, is over-design against seismic loadings. Thus, we can also state that the coefficient of 5 ‰ used to prescribe the allowable lateral top drift is too large and that we should instead use a coefficient of 3.3 ‰. Now, if we consider that the level of risk acceptability is 8.2×10^{-3}, which corresponds to the target reliability index $\beta = 2.4$ as proposed by Hirataï and Ishikawa [31], the allowable maximum lateral drift becomes 27 mm and we should use a coefficient of 3 ‰. Finally, if degree of inspectability, reparability and damage tolerance is low, EC0 specifies a target reliability index $\beta = 3.8$ for fatigue or cyclic loadings (which corresponds to $P_f =$

7.2×10^{-5}) and, in this case, allowable lateral top drift must be 22 mm and a conservative coefficient of 2.4 ‰ must be used instead of initial value of 5 ‰.

6. Conclusions

In the present work, effectiveness of externally bonded FRP-strengthening on the seismic fragility of RC frame was examined. Two different FRP-strengthening techniques was considered; FRP columns confining and/or FRP flexural/confining. To obtain an explicit response formula, a second-order PDD based on quadratic Gauss-Hermite numerical integration was used. It is shown that Polynomial Dimension Decomposition response surface methodology not only can robustly predict the desired response, but also can simplify the process of fragility computation. Sobol Sensitivity indices were evaluated for each of the random variables. It has been shown that concrete compressive strength, dead load, live load and model error are the most important variables in the reliability analysis. In contrast, small values of Sobol indices were recorded for steel modulus, steel strength, damping ratio and FRP properties. Later variables are strongly to be deterministic variables in future studies. In addition, the partial safety factors associated to these parameters can be neglected in the empirical models used in the design codes, which can simplify considerably the computational efforts in the design process.

Compared to traditional deterministic models, probabilistic analysis gives additional information about the variability of the damage accumulated in the structure, which defined here as the lateral top drift. Indeed, as presented below, from the probability density function plots we can easily identify the region where is located the major mass of probability contents, in other word the location of the most probable failure events. As can be seen from figure 10, the lateral top drift probability mass is localised in the tail of the distribution instead of the neighbourhood of the mean value. This information is very useful to the designers which can focus their efforts only on the most probable failure events.

Fragility curves, which can be used as design charts, were estimated using Monte-Carlo simulation based on the polynomial surface response function obtained. One can note that, these fragility curves are obtained without additional calls of the implicit mechanical model, which strongly reduce the computation times. It is remarkable to observe that both the considered FRP strengthening techniques can enhance seismic fragility

curves. However, FRP-flexural strengthening effect was found to be the most dominant as its effect reduce the damage probability by a factor two.

The proposed reliability procedure is considered as an initial step towards the evolution of seismic reliability of FRP-strengthened RC frames. It is suggested to consider additional seismic aspects such as: variability in seismic motion, soil type, shear-at-base/spectral-acceleration ultimate limit states…etc. Such these aspects can generalize the obtained results. In addition, spatial variability of concrete compressive strength of the different elements of the RC frame may show a valuable change in fragility curves.

7. *References*

[1] American Concrete Institute Committee 440. ACI 440.2R-17: Guide for the design and construction of externally bonded FRP system for strengthening concrete structures. Farmington Hills, MI: ACI 2017. 112 pages. ISBN: 9781945487590.

[2] Ali O, Bigaud D, Ferrier E. Comparative durability analysis of CFRP-strengthened RC highway bridges. Journal of Construction and Building Materials 2012; 30:629–642. doi.org/10.1016/j.conbuildmat.2011.12.014.

[3] Correia L, Sena-Cruz J, Michels J, França P, Escusa G. Durability of RC slabs strengthened with prestressed CFRP laminate strips under different environmental and loading conditions. Compos Part B Eng 2017; 125:71-88. doi.org/10.1016/j.compositesb.2017.05.047.

[4] Khalifa ES, Al-Tersawy SH. Experimental and analytical investigation for enhancement of flexural beams using multilayer wraps. Compos Part B Eng 2013; 45:1432–40. doi:10.1016/j.compositesb.2012.08.021.

[5] Mosallam AS, Nasr A. Structural performance of RC shear walls with post-construction openings strengthened with FRP composite laminates. Compos Part B Eng 2017; 115:488-504. doi.org/10.1016/j.compositesb.2016.06.063.

[6] Qin R, Zhou A, Lau D. Effect of reinforcement ratio on the flexural performance of hybrid FRP reinforced concrete beams. Compos Part B Eng 2017; 108(1) 200–09. doi.org/10.1016/j.compositesb.2016.09.054.

[7] Triantafyllou GG, Rousakis TC, Karabinis AI. Corroded RC beams patch repaired and strengthened in flexure with fiber-reinforced polymer laminates. Compos Part B Eng 2017; 112:125-36. doi.org/10.1016/j.compositesb.2016.12.032.

[8] Giamundo V, Lignola G P, Fabbrocino F, Prota A, Manfredi G. Influence of FRP wrapping on reinforcement performances at lap splice regions in RC columns. Compos Part B Eng 2017; 116:313-24. doi.org/10.1016/j.compositesb.2016.10.069.

[9] Belarbi A, Bae SW. An experimental study on the effect of environmental exposures and corrosion on RC columns with FRP composite jackets. Compos Part B Eng B 2007; 38:674–84. doi:10.1016/j.compositesb.2006.09.004.

[10] Lignola GP, Nardone F, Prota A, Manfredi G. Analytical model for the effective strain in FRP-wrapped circular RC columns. Compos Part B Eng 2012; 43:3208–18. doi.org/10.1016/j.compositesb.2012.04.007.

[11] Ghorbi E, Soltani M, Maekawa K. Development of a compressive constitutive model for FRP-confined concrete elements. Compos Part B Eng 2013; 45:504–17. doi.org/10.1016/j.compositesb.2012.07.014.

[12] Abbasnia R, Ahmadi R, Ziaadiny H. Effect of confinement level, aspect ratio and concrete strength on the cyclic stress-strain behavior of FRP-confined concrete prisms. Compos Part B Eng 2012; 43:825–31. doi.org/10.1016/j.compositesb.2011.11.008.

[13] Charalambidi BG, Rousakis TC, Karabinis AI. Analysis of the fatigue behavior of reinforced concrete beams strengthened in flexure with fiber reinforced polymer laminates. Compos Part B Eng 2016; 96:69-78. doi.org/10.1016/j.compositesb.2016.04.014.

[14] Mukherjee A, Joshi M. FRPC reinforced concrete beam column joints under cyclic excitation. Journal of Composite Structures 2005; 70:185-99. doi.org/10.1016/j.compstruct.2004.08.022.

[15] Binici B, Ozcebe G, Ozcelik R. Analysis and design of FRP composites for seismic retrofit of infill walls in reinforced concrete frames. Compos Part B Eng 2007; 38:575–83. doi:10.1016/j.compositesb.2006.08.007.

[16] Zou XK, Teng JG, De Lorenzis L, Xia SH. Optimal performance-based design of FRP jackets for seismic retrofit of reinforced concrete frames. Compos Part B Eng 2007; 38:584–97. doi:10.1016/j.compositesb.2006.07.016.

[17] Dan D. Experimental tests on seismically damaged composite steel concrete walls retrofitted with CFRP composites. Engineering Structures 2012; 45:338-348. doi.org/10.1016/j.engstruct.2012.06.037.

[18] Del Zoppo M, Di Ludovico M, Balsamo A, Prota A, Manfredi G. FRP for seismic strengthening of shear controlled RC columns: Experience from earthquakes and experimental analysis. Compos Part B Eng 2017; 129:47-57. doi.org/10.1016/j.compositesb.2017.07.028.

[19] Di Ludovico M, Prota A, Manfredi G, Cosenza E. Seismic behavior of full-scale RC structures using GFRP laminates. Journal of Structural Engineering 2008; 134(5):810-21. doi.org/10.1061/(ASCE)0733-9445(2008)134:5(810).

[20] Garcia R, Hajirasouliha I, Pilakoutas K. Seismic behavior of deficient RC frames strengthened with CFRP composites. Engineering Structures 2010; 32:3075-85. doi.org/10.1016/j.engstruct.2010.05.026.

[21] Eslami A, Ronagh HR. Effect of FRP wrapping in seismic performance of RC buildings with and without special detailing - A case study. Compos Part B Eng 2013; 45:1265–74. doi.org/10.1016/j.compositesb.2012.09.031.

[22] Bilotta A, Faella C, Martinelli E and Nigro E. Design by testing procedure for intermediate debonding in EBR FRP strengthened RC beams. Engineering Structures 2013; 46: 147-154. doi.org/10.1016/j.engstruct.2012.06.031.

[23] Atadero AA, Karbhari VM. Calibration of resistance factor for reliability based design of externally-bonded FRP composites. Compos Part B Eng B 2008; 39(4):665-79. doi: 10.1016/j.compositesb.2007.06.004.

[24] Bigaud D, Ali O. Time-variant flexural reliability of RC beams with externally bonded CFRP under combined fatigue-corrosion actions. Reliability Engineering and System Safety 2014; 131:257-270. doi.org/10.1016/j.ress.2014.04.016.

[25] Corradi M, Borri A, Righetti L, Speranzini E. Uncertainty analysis of FRP reinforced timber beams. Compos Part B Eng 2017; 113:174-184. doi.org/10.1016/j.compositesb.2017.01.030.

[26] Lemaire M, Chateauneuf A, Mitteau J. Structural Reliability. Chapter 5. Reliability index. United States: John Wiley & Sons Ltd; 2009. doi.org/10.1002/9780470611708.ch5.

[27] Riahi H. Analyse de structures à dimension stochastique élevée: application aux toitures bois sous sollicitation sismique. (Doctoral dissertation), University of BLAISE PASCAL - CLERMONT II, France; 2013. (in French).

[28] Kwon O, Elnashai A. The effect of material and ground motion uncertainty on the seismic vulnerability of RC structure. Engineering Structures 2006; 28(2):289–303. doi.org/10.1016/j.engstruct.2005.07.010.

[29] Ramamoorthy S, Gardoni P, Bracci J. Probabilistic demand models and fragility curves for reinforced concrete frames. Journal of Structural Engineering 2006; 132(10):1563–72. doi.org/10.1061/(ASCE)0733-9445(2006)132:10(1563).

[30] Buratti N, Ferracuti B, Savoia M. Response Surface with random factors for seismic fragility of reinforced concrete frames. Journal of Structural Safety 2010; 32:42–51. doi.org/10.1016/j.strusafe.2009.06.003.

[31] Kumar R, Gardoni P. Effect of seismic degradation on the fragility of reinforced concrete bridges. Engineering Structures 2014; 79:267-275. doi.org/10.1016/j.engstruct.2014.08.019.

[32] Monteiro R. Sampling based numerical seismic assessment of continuous span RC bridges. Engineering Structures 2016; 118:407-420. doi.org/10.1016/j.engstruct.2016.03.068.

[33] Ramamoorthy SK, Gardoni P, Bracci J. Seismic fragility and confidence bounds for gravity load designed reinforced concrete frames of varying height. Journal of Structural Engineering 2008; 134(4):639–50. doi.org/10.1061/(ASCE)0733-9445(2008)134:4(639).

[34] Eurocode 8. Design of structures for earthquake resistance, Part 1: General rules, seismic actions and rules for buildings 2003.

[35] Vu K, Stewart MG. Structural reliability of concrete bridges including improved chloride-induced corrosion models. Journal of Structural Safety 2000 ;22:313-333. doi.org/10.1016/S0167-4730(00)00018-7.

[36] Eurocode 0. Basis of structural design, Annex C : Basis for partial factor design and reliability analysis 2005.

[37] Hiratai K. and Ishikawa T. 2004. Probabilistic evaluation of desirable target seismic level derived from requirements of users, 13th World Conference on Earthquake Engineering - Vancouver, B.C., Canada, August 1-6, 2004- Paper No. 219.

[38] Wang L, Wu Y. Effect of corner radius on the performance of CFRP-confined square concrete columns: Test. Journal of Engineering Structures 2008; 30:493–505. doi.org/10.1016/j.engstruct.2007.04.016.

[39] Sharma S, Dave U, Solanki H. FRP Wrapping for RC Columns with Varying Corner Radii. Journal of Procedia Engineering 2013; 51:220–29. doi.org/10.1016/j.proeng.2013.01.031.

[40] T. El-Maaddawy, 2008. Behavior of corrosion-damaged RC columns wrapped with FRP under combined flexural and axial loading. Cement & Concrete Composites 30; 524-534. doi.org/10.1016/j.cemconcomp.2008.01.006.

[41] J. Teng, J. Chen, S. Smith and L. Lam, 2001. FRP-strengthened RC structures. England, John Wiley & Sons Ltd. 266 pages. ISBN: 978-0-471-48706-7

[42] CEB-FIP Model Code 1990. London: Thomas Telford Services Ltd; 2008. 437 pages. ISBN: 9780727735430.

[43] Coronado CA, Lopez MM. Sensitivity analysis of reinforced concrete beams strengthened with FRP laminates. Journal of Cement & Concrete Composites 2005;28:102-14. doi.org/10.1016/j.cemconcomp.2005.07.005.

[44] ABAQUS Theory Manual, User Manual and Example Manual, Version 6.12, Providence, RI. 2012.

[45] Chopra AK. Dynamic of Structures - Theory and Application to Earthquake Engineering (fifth edition). United States : Prentice-Hall Inc; 2016. 992 pages. ISBN-10: 0134555120.

[46] Nataf A. Détermination des distributions dont les marges sont données. Comptes Rendus de l'Académie des Sciences. Paris 1962; 225:42-43. (in French).

[47] Rahman S. A polynomial dimensional decomposition for stochastic computing. International journal for numerical method in engineering 2008; 76:2091-2116. doi.org/10.1002/nme.2394.

[48] Xu H, Rahman S. A generalized dimension-reduction method for multidimensional integration in stochastic mechanics. Journal for Numerical Methods in Engineering 2004; 61:1992-2019. doi.org/ 10.1002/nme.1135.

[49] Sobol M. Sensitivity estimates for non-linear mathematical models. Matematicheskoe Modelirovanie, Vol. 2, No. 1, 1990, pp.112–118 (in Russian), English translation in Mathematical Modelling and Computational Experiment, Vol. 1, No. 4, 1993, pp. 407–414.

[50] Homma T, Saltelli A. Importance measures in global sensitivity analysis of non-linear models. Journal of Reliability Engineering and System Safety 1996; 52:1-17. doi.org/10.1016/0951-8320(96)00002-6.

[51] The Joint Committee on Structural Safety (JCSS). Probabilistic model code; 2001. ISBN 978-3-909386-79-6.

Seismic performance of reinforced concrete frame structures strengthened with FRP laminates using a reliability-based advanced approach
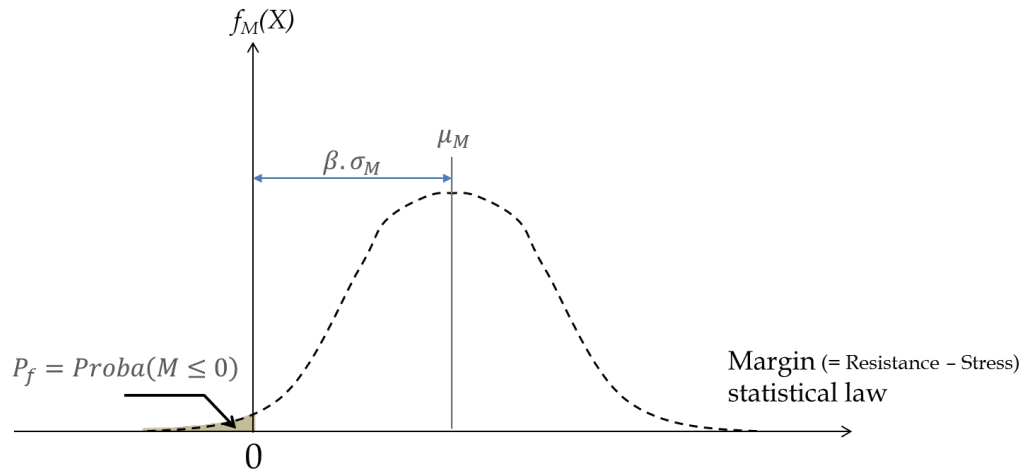
Figures

Figure 1: Naïve illustration of two reliability indicators.
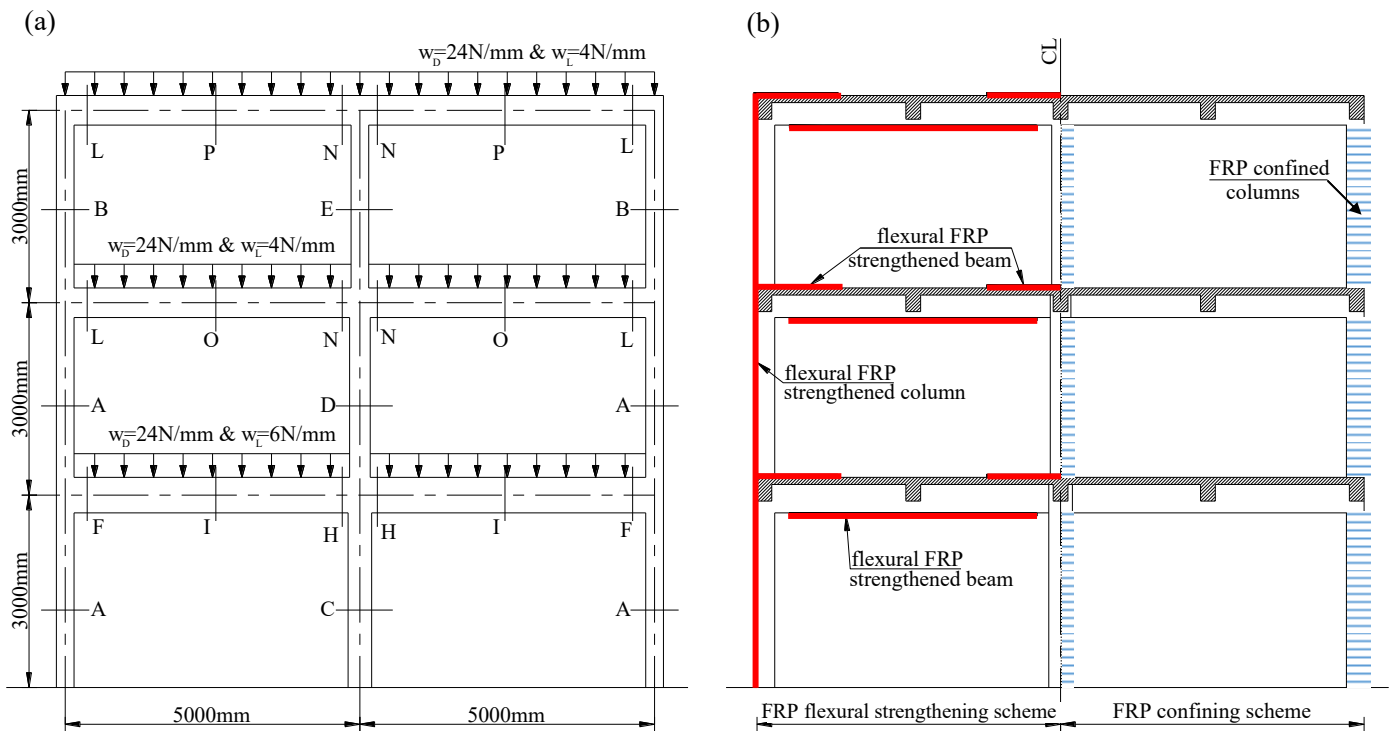

Figure 2: a) Three-storey RC Frame configuration (from [23]). b) considered FRP strengthening schemes.
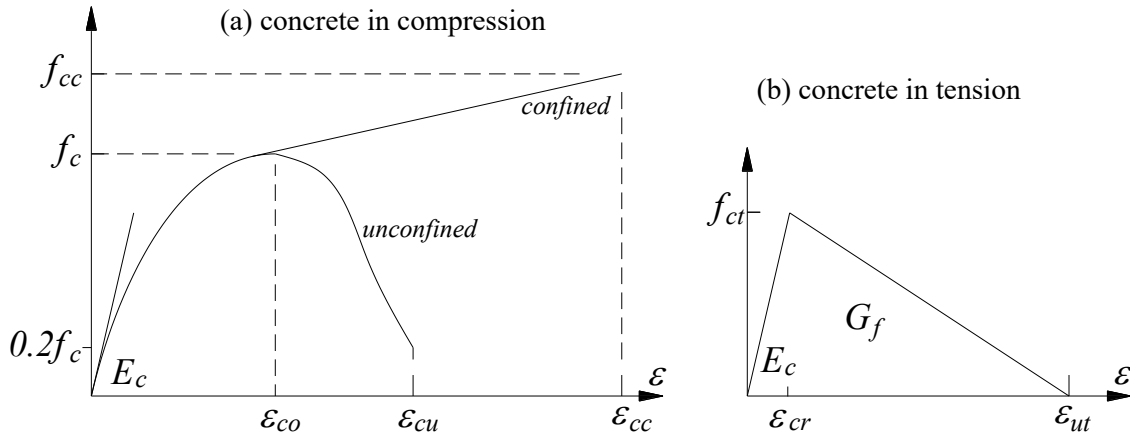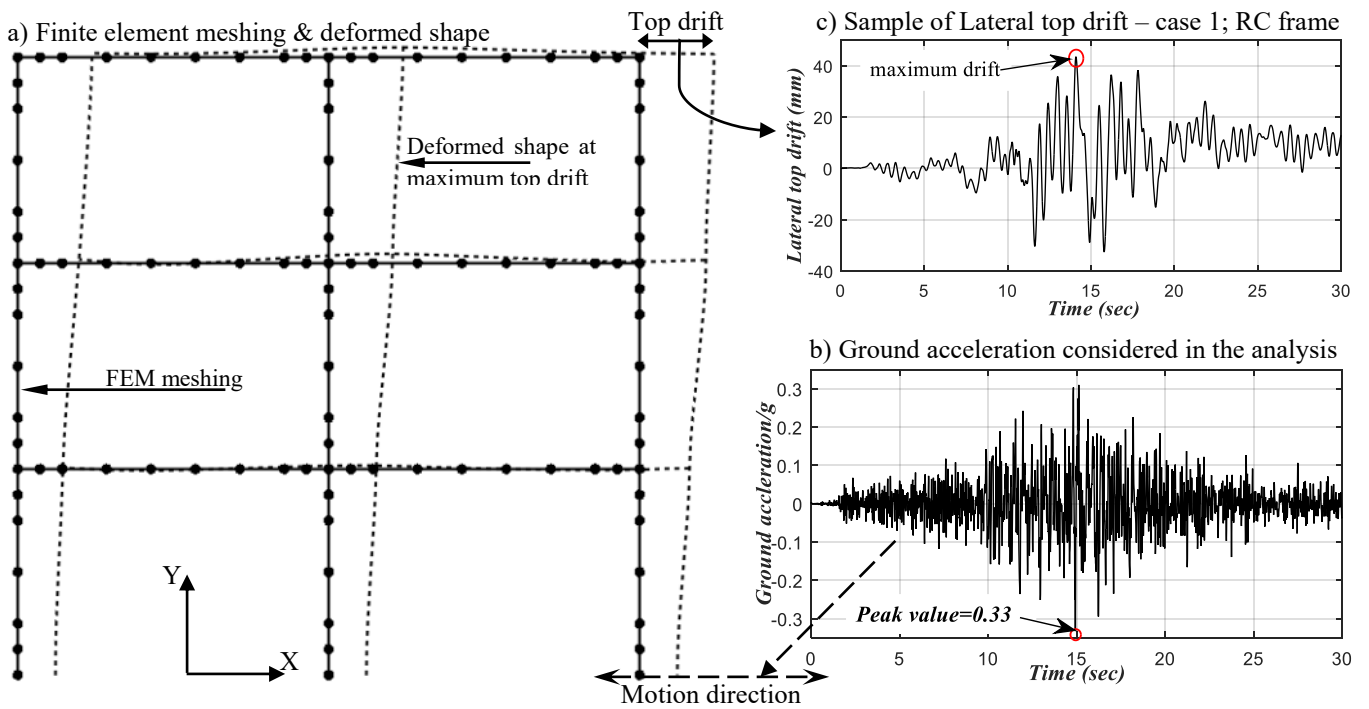
Figure 3: Concrete stress-strain curves.

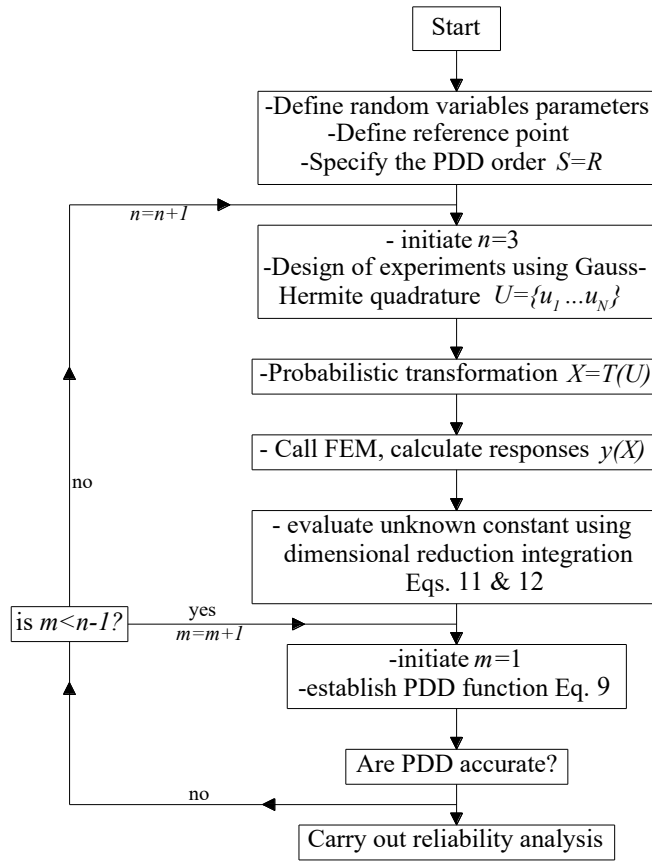Figure 4: a) FEM meshing, b) applied ground acceleration and c) sample of lateral top drift results.

Start

-Define random variables parameters
-Define reference point
-Specify the PDD order $S=R$

$n=n+1$

- initiate $n=3$
-Design of experiments using Gauss-Hermite quadrature $U=\{u_1...u_N\}$

-Probabilistic transformation $X=T(U)$

- Call FEM, calculate responses $y(X)$

- evaluate unknown constant using dimensional reduction integration Eqs. 11 & 12

is $m<n-1$?

yes
$m=m+1$

-initiate $m=1$
-establish PDD function Eq. 9

no

Are PDD accurate?

no

Carry out reliability analysis

Figure 5: Computational procedure for the establishment of dimensional polynomial decomposition function.
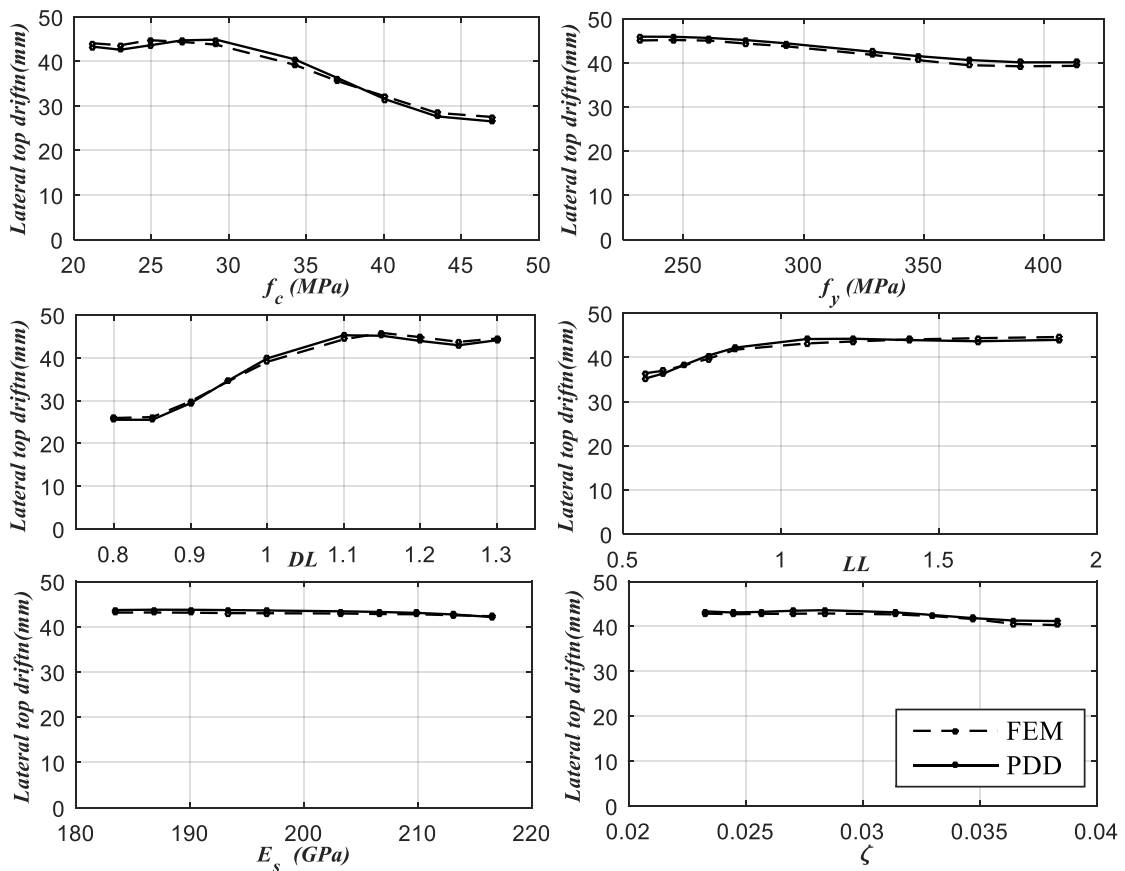
Figure 6: Validation of polynomial dimensional decomposition PDD function.
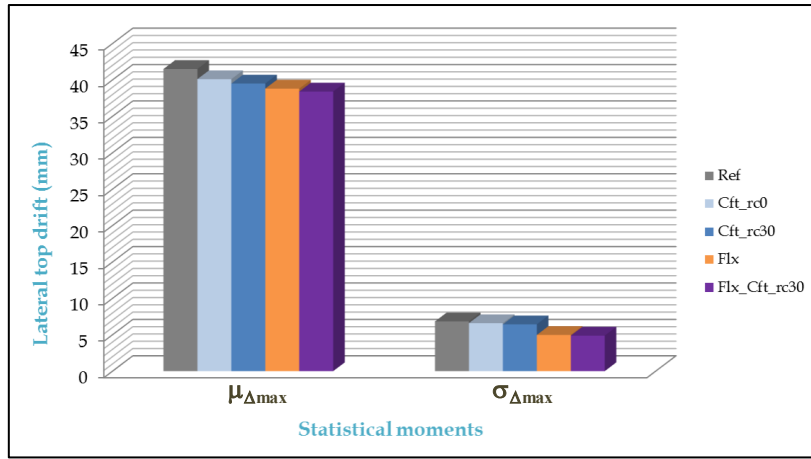
Figure 7: Mean and standard deviation of lateral top drift (mm) of the different cases considered.
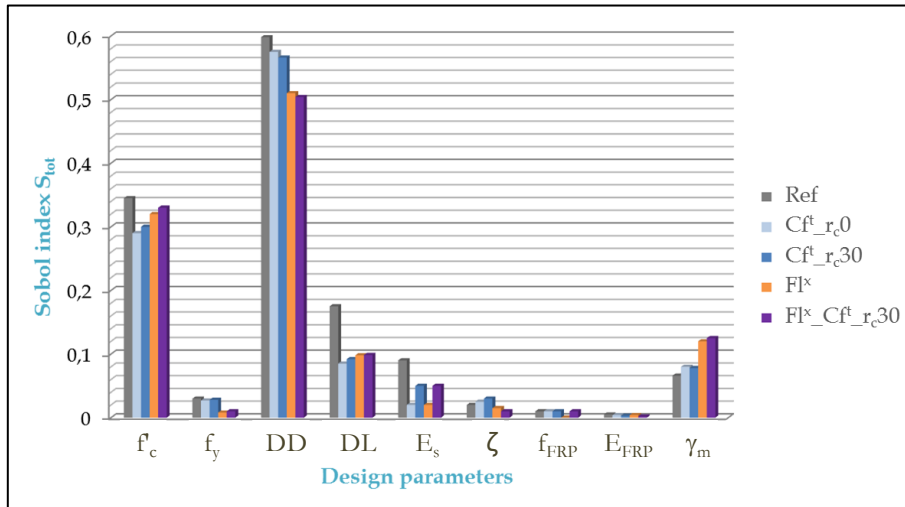

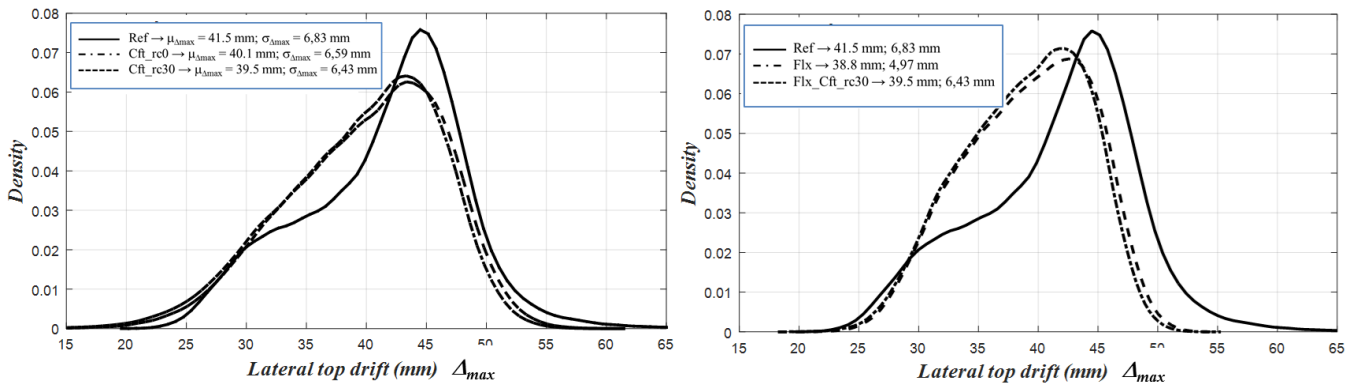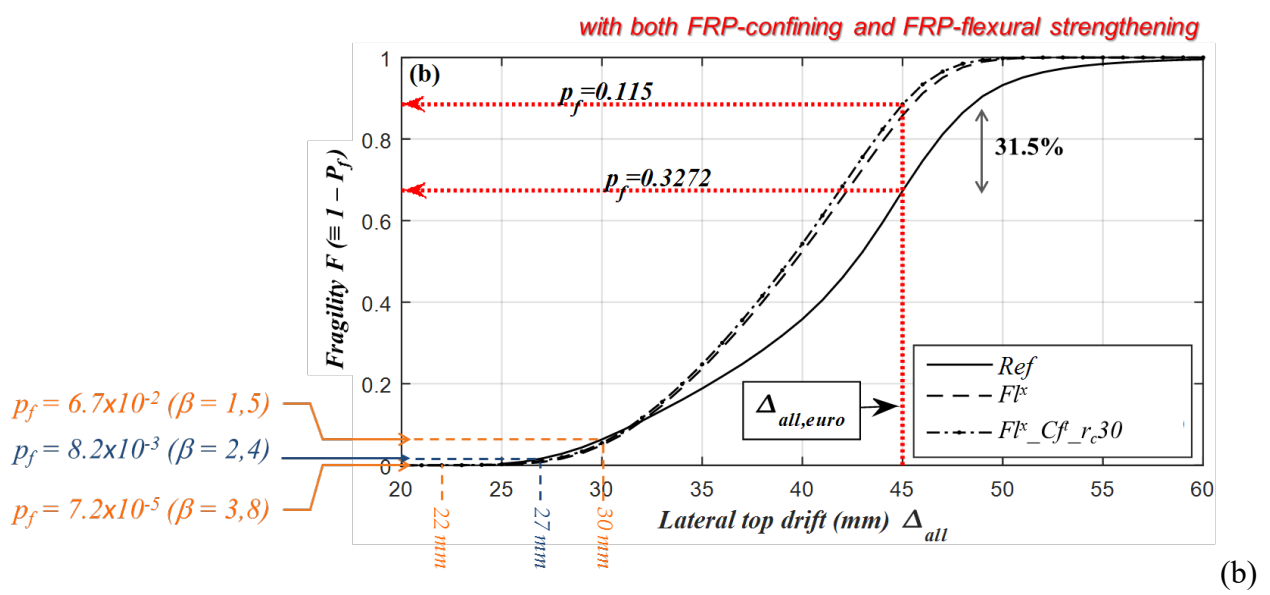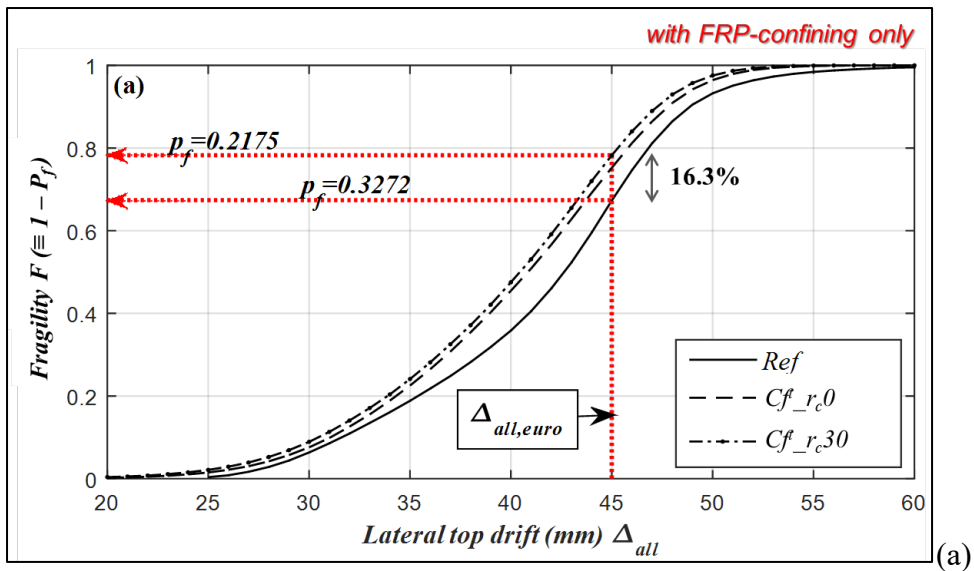*Figure 8: Sobol sensitivity indices of random variables included in PDD function.*

Figure 9: Density function PDF of lateral top drift Δ_{max} (mm).

Figure 10: Fragility curves.

Seismic performance of reinforced concrete frame structures strengthened with FRP laminates using a reliability-based advanced approach

Tables

Table 1: Cross-sections geometry of RC frame

Section	Width (mm)	Height (mm)	A_s	A_s'
A	300	300	2ϕ20mm	2ϕ20mm
B	300	300	3ϕ20mm	3ϕ20mm
C	400	400	2ϕ18mm	2ϕ18mm
D	350	350	2ϕ18mm	2ϕ18mm
E	300	300	2ϕ18mm	2ϕ18mm
F	300	600	2ϕ18mm	2ϕ18mm
I	300	600	2ϕ18mm+2ϕ20mm	2ϕ18mm
H	300	600	2ϕ18mm+1ϕ20mm	2ϕ18mm+4ϕ20mm
L	300	500	2ϕ18mm	3ϕ18mm
O	300	500	5ϕ18mm	2ϕ18mm
N	300	500	2ϕ18mm+3ϕ20mm	2ϕ18mm+4ϕ20mm
P	300	500	2ϕ18mm+3ϕ20mm	2ϕ18mm

Table 2: Description of the studied cases.

Cases	Description	FEM calls required for construction of PDD
Ref	RC frame which is the reference/control case.	266
Cf_rc0	RC frame applying FRP confinement strengthening with a corner radius r_c=zero.	366
Cf_rc30	RC frame applying FRP confinement strengthening with r_c=30mm.	366
Flx	RC frame applying FRP flexural strengthening.	366
Flx_Cf_rc30	RC frame applying both FRP flexural and FRP confinement strengthening with r_c=30mm.	482

Table 3: Probabilistic parameters of random variables.

Variable	Distribution	Units	Mean value (μ)	Standard deviation (σ)	Notes
Concrete strength f'_c	Log-normal	MPa	32	5.12	---
Steel yield stress f_y	Log-normal	MPa	312	36.2	---
Error in dead load DL	Normal	---	1.05	0.10	Multiplied by Nominal dead load (w_D)
Error in live load LL	GEV	---	1.0	0.25	Multiplied by Nominal live load (w_L)
Steel Modulus E_s	Normal	MPa	200000	6600	---
Damping ratio ζ	Log-normal	---	0.03	0.003	---
FRP strength f_{FRP}	Weibull	MPa	900	135	---
FRP modulus E_{FRP}	Log-normal	GPa	75	150	---
Error in FRM γ_m	Normal	---	1.01	0.046	---